

RESEARCH ARTICLE | FEBRUARY 28 2023

## Compact optomechanical accelerometers for use in gravitational wave detectors

Special Collection: [Gravitational Wave Detectors](#)

A. Hines  ; A. Nelson  ; Y. Zhang  ; G. Valdes  ; J. Sanjuan  ; F. Guzman  

 Check for updates

*Appl. Phys. Lett.* 122, 094101 (2023)

<https://doi.org/10.1063/5.0142108>



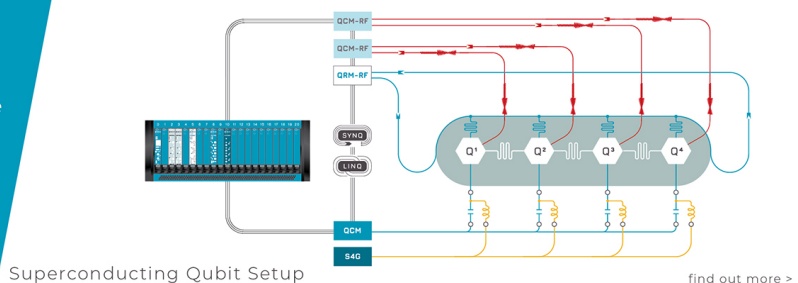
View  
Online



Export  
Citation

CrossMark

 **QBLOX**  
Integrates all  
Instrumentation + Software  
for Control and Readout of  
**Superconducting Qubits**  
**NV-Centers**  
**Spin Qubits**



# Compact optomechanical accelerometers for use in gravitational wave detectors

Cite as: Appl. Phys. Lett. **122**, 094101 (2023); doi: [10.1063/5.0142108](https://doi.org/10.1063/5.0142108)

Submitted: 11 January 2023 · Accepted: 16 February 2023 ·

Published Online: 28 February 2023



View Online



Export Citation



CrossMark

A. Hines, A. Nelson, Y. Zhang, G. Valdes, J. Sanjuan, and F. Guzman<sup>a)</sup>

## AFFILIATIONS

Aerospace Engineering and Physics, Texas A&M University, College Station, Texas 77843, USA

**Note:** This paper is part of the APL Special Collection on Gravitational Wave Detectors.

<sup>a)</sup>Author to whom correspondence should be addressed: [felipe@tamu.edu](mailto:felipe@tamu.edu)

## ABSTRACT

We present measurements of an optomechanical accelerometer for monitoring low-frequency noise in gravitational wave detectors, such as ground motion. Our device measures accelerations by tracking the test-mass motion of a 4.7 Hz mechanical resonator using a heterodyne interferometer. This resonator is etched from monolithic fused silica, an under-explored design in low-frequency sensors, allowing a device with a noise floor competitive with existing technologies but with a lighter and more compact form. In addition, our heterodyne interferometer is a compact optical assembly that can be integrated directly into the mechanical resonator wafer to further reduce the overall size of our accelerometer. We anticipate this accelerometer to perform competitively with commercial seismometers, and benchtop measurements show a noise floor reaching 82 pico-g Hz<sup>-1/2</sup> sensitivities at 0.4 Hz. Furthermore, we present the effects of air pressure, laser fluctuations, and temperature to determine the stability requirements needed to achieve thermally limited measurements.

Published under an exclusive license by AIP Publishing. <https://doi.org/10.1063/5.0142108>

Ground-based gravitational wave detectors, such as LIGO,<sup>1</sup> VIRGO,<sup>2</sup> and KAGRA,<sup>3</sup> famously require laser interferometers with displacement sensitivities better than  $10^{-19} \text{ m}/\sqrt{\text{Hz}}$  over a bandwidth of tens to hundreds of Hz, achieved through large test masses with low thermal noise and a high degree of seismic isolation.<sup>4</sup> However, even with these advancements, gravitational wave detectors are still susceptible to low-frequency ground motion, both seismic and anthropogenic in origin.<sup>5–9</sup> This in turn requires extensive physical environmental monitoring of the ambient conditions and ground motion for use in various watchdogs, warning systems, active feedback controls, and data post-corrections. For this, the detectors use many high-sensitivity displacement sensors, geophones, accelerometers, and seismometers. However, commercially available seismometers currently employed have some flaws, including their large dimensions and weights and their inherent vacuum incompatibility, which adds hurdles that must be overcome before they can be deployed inside vacuum chambers.

In this Letter, we present our low-frequency optomechanical accelerometer that could be used to characterize seismic noise and effects in gravitational wave detectors. This accelerometer uses an optical readout scheme for tracking the mechanical resonator test mass motion, from which we recover ambient accelerations that couple into the sensor.

The mechanical resonator is etched from one wafer of monolithic fused silica, designed to be easily integrated with a compact heterodyne interferometer. This design allows for a much smaller form than other seismometer technologies, with fewer components and lower susceptibility to mechanical instabilities. Our optomechanical accelerometer is vacuum-compatible, allowing easier deployment in the chambers enclosing the gravitational-wave detectors.

Our design features optical readouts, in contrast to commercial seismometers that typically use electrostatic readouts susceptible to environmental noises. Moreover, the sub-Hz measurement regime is an under-explored design space for optomechanical devices typically used for high-frequency applications. A similar glass oscillator accelerometer has demonstrated a thermally limited acceleration noise floor of  $100 \text{ ngHz}^{-1/2}$  over a 10 kHz operating bandwidth.<sup>10</sup> Lower frequency fused silica accelerometers have shown high mechanical Q-factors on the order of  $10^5$ , though the thermally limited noise floors have yet to be experimentally observed.<sup>11,12</sup> In this Letter, we present the design of our accelerometer (a mechanical resonator and optical readout), noise floor measurements, and the sensitivity noises induced through ambient disturbances and laser instability.

The mechanical resonator we use for detecting accelerations is laser-assisted dry-etched from a monolithic fused silica wafer. This wafer is  $90 \times 80 \times 6.6 \text{ mm}^3$  in size and 58.2 g in weight, while the test

mass is 2.6 g in weight. The test mass is supported by two 100  $\mu\text{m}$ -thick leaf-spring flexures that yield a resonant frequency of 4.7 Hz. A computational analysis of the mechanical losses of fused silica was performed to estimate the flexure dimensions and test mass, which minimize the self-noise of our accelerometer with a resonance frequency on the order of 1 Hz. A natural frequency in this band is desirable for maximizing the test mass response to sub-Hz signals. Specifically, below resonance, the test mass response  $x$  to an acceleration signal  $a$  is approximated by

$$x \approx \frac{a}{\omega_0^2}, \quad (1)$$

where  $\omega_0$  is the resonant frequency. Hence, a low-frequency resonator is appropriate for low-frequency signal detection.

A rendering of our resonator is shown in Fig. 1. When laid in the orientation shown in this photo, the test mass oscillates in the horizontal plane from left-to-right. Rotating the wafer so that the test mass oscillates vertically would allow for  $z$ -axis acceleration measurements. Finally, cutouts on the wafer allow for the implementation of a compact interferometer unit that tracks the test mass motion onto the fused silica itself, which is advantageous for maintaining a compact form.

The displacement of the test mass from equilibrium is measured by a compact, quasi-monolithic heterodyne interferometry unit. Other works provide an in-depth discussion of this unit,<sup>13</sup> though an overview is provided here. A fiber-coupled 1064 nm laser source is split in two, with each beam frequency shifted by acousto-optical modulators (AOMs) to create a 1 MHz beatnote. Both beams are injected into the optical assembly, which further splits beams to create two laser interferometers: a measurement interferometer and a reference interferometer. Between both interferometers, there are four beams, which reflect off of three different mirrors. One mirror that is attached to the quasi-monolithic optical assembly itself is common to both interferometers. The second beam of the measurement interferometer reflects off of a mirror on the test mass, allowing it to track the test mass motion.

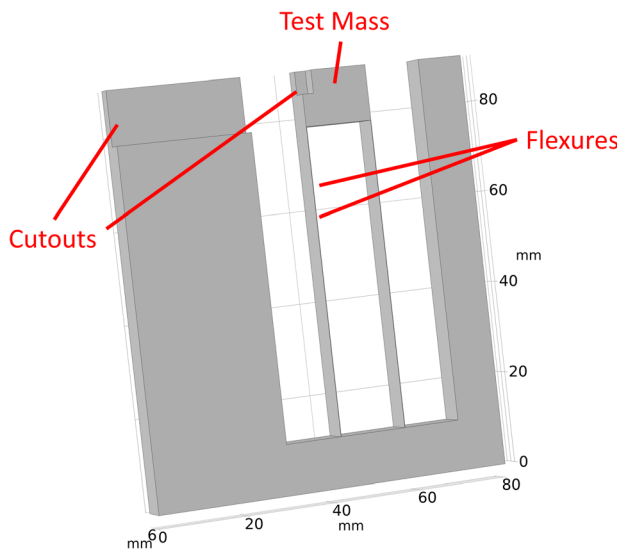


FIG. 1. COMSOL rendering of our 5 Hz resonator.

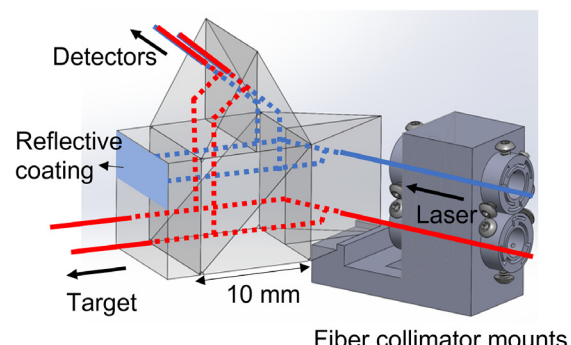


FIG. 2. Diagram of our quasi-monolithic interferometer unit. This optical assembly uses a differential phase measurement of two heterodyne interferometers: a measurement interferometer and a reference interferometer. The red and blue traces show the paths of two frequency-shifted laser beams. The blue trace reflects off a reflective coating on the quasi-monolithic interferometer before interfering with the red trace. The laser beams in red are sent to a mirror on the test mass and a stationary mirror on the fused silica wafer.

Similarly, the second beam of the reference interferometer reflects off of a stationary mirror on the wafer of the resonator. A differential phase measurement of the two interferometers yields a test mass displacement measurement which rejects common-mode noise. A diagram of this optical unit is shown in Fig. 2. Our quasi-monolithic interferometer has a  $10 \times 18 \text{ mm}^2$  footprint, allowing it to be easily integrated onto the wafer of our optomechanical accelerometer. By maintaining a compact form, we reduce noise in our acceleration measurements originating from thermal expansion, which has been previously identified as a dominating noise source in the sub-Hz regime.<sup>12</sup> A photograph of the quasi-monolithic interferometer and fused silica resonator in our experimental setup is shown in Fig. 3.

Moreover, fused silica as a wafer material is chosen for its low intrinsic losses which yield a low self-noise in the resonator.<sup>11,14,15</sup> This in turn lowers the noise floor of our prototype accelerometer and provides better acceleration sensitivity. The performance of our

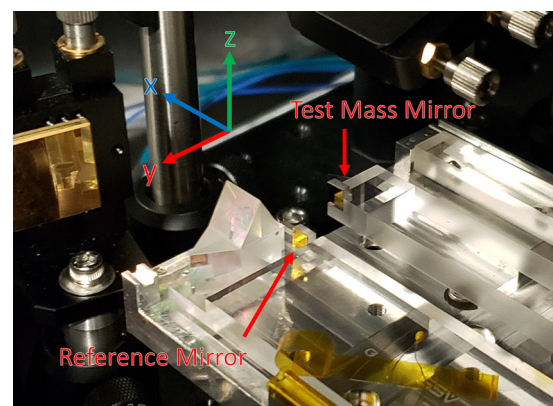


FIG. 3. Photograph of our resonator with the quasi-monolithic interferometer integrated onto the fused silica wafer, highlighting the locations of the reference and test mass mirrors. In this photo, two frequency-shifted beams enter the interferometer unit from the left side and exit toward the top-right corner.

optomechanical accelerometer is fundamentally limited by the thermal motion of the fused silica resonator, which is related to the mechanical quality factor  $Q$  of the resonator. We plot the thermal acceleration noise of our device in Fig. 4, assuming a theoretical analysis of the mechanical losses in the fused silica<sup>11</sup> and a  $Q$ -value of  $4.77 \times 10^5$  in vacuum at  $\mu\text{Torr}$  pressures, measured experimentally by ringdown.<sup>12</sup> The theoretical noise floor is calculated considering bulk effects, surface effects, and thermoelastic effects to be the dominant energy dissipation mechanisms within the fused silica.<sup>11,14,15</sup> The discrepancy between the theoretical and measured  $Q$ -values is believed to originate from surface roughness and defects created during fabrication. Hence, annealing the fused silica resonators is expected to improve our measured quality factors.<sup>16</sup>

Also shown in Fig. 4 is the self-noise of the GS-13 seismometer, which was experimentally measured by members of the LIGO Scientific Collaboration.<sup>17</sup> We note that the acceleration noise floor of our optomechanical accelerometer is expected to be competitive with, if not better than, these commercial devices. The GS-13, for reference, is deployed in the vacuum chambers of gravitational wave detectors for ground motion detection. This suggests that our optomechanical device is a viable alternative to the seismometers currently used by LIGO.

Due to the ultra-low frequency bandwidth we are targeting with our accelerometer, achieving a seismic isolation sufficient to directly measure the self-noise of our device is extremely demanding and impractical. Data taken with our accelerometer will necessarily be dominated by ground motion. Hence, we test the performance of our optomechanical accelerometer by taking a 14-h measurement of the ambient seismic noise and comparing against a reference commercial seismometer. This seismometer is placed in close proximity to our accelerometer to ensure long-period seismic signals couple into both devices coherently. In addition, the axis of motion of the resonator is aligned to the  $y$ -axis of the seismometer, allowing for simple comparison of the two sensors. Moreover, fluctuations in the ambient conditions, including temperature, air pressure, and laser frequency, add substantial noise that further masks the noise floor of our

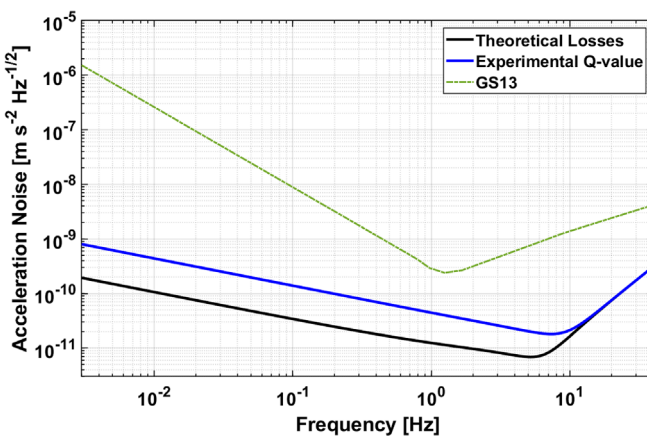


FIG. 4. Plot of the thermally limited acceleration noise floor of our optomechanical accelerometer based on both theoretical dissipation mechanisms<sup>11</sup> and an experimental value of the mechanical quality factor.<sup>12</sup> These are compared to the self-noise of the GS-13 seismometer.<sup>17</sup>

accelerometer. Laser frequency fluctuations couple into our acceleration measurements as noise via the optical path length difference between the measurement and reference interferometers. We make a simultaneous observation of this laser frequency noise using a fiber-based delay-line interferometer, which allows us to calculate the laser frequency noise coupling coefficient and remove this effect from our acceleration data. Similarly, the ambient temperature and pressure fluctuations are measured using off-the-shelf thermistors and barometers in order to estimate the noise contributions from those fluctuations.

The amplitude spectral densities of our optomechanical accelerometer data as well as the contributions from seismic motion, laser frequency noise, temperature fluctuations, and barometric pressure are shown in Fig. 5. We observe that the raw data are dominated by ground motion signals and laser frequency fluctuations above 1 MHz, with appreciable contributions from temperature and pressure noise. All noise contributions are estimated through a frequency-domain transfer function method.<sup>12</sup> The residual noise after removing all contributions reaches an acceleration sensitivity of  $10 \text{ nm s}^{-2} \text{ Hz}^{-1/2}$  at 0.4 Hz, nearly two orders of magnitude lower than the ambient ground motion.

Moreover, we repeat this experiment with the test mass anchored in place to estimate the current acceleration noise floor of our laser interferometric readout. We preload the test mass and flexures by inserting a piece of fused silica between the test mass and the frame of the resonator, which prevents the resonator from moving in response to accelerations. The spectral densities of a 14-h measurement with our setup in this configuration is shown in Fig. 6 where we note significant contributions from temperature, and laser frequency fluctuations. These contributions are identified and removed in the same way as before to find an acceleration noise of  $0.8 \text{ nm s}^{-2} \text{ Hz}^{-1/2}$  at 0.4 Hz, more than an order of magnitude lower than was observed with the test mass free to oscillate. This acceleration noise is equivalent to a test mass displacement noise of  $0.9 \text{ pm Hz}^{-1/2}$ .

Because the optomechanical accelerometer did not sense the ground motion and effects from the environment and laser source

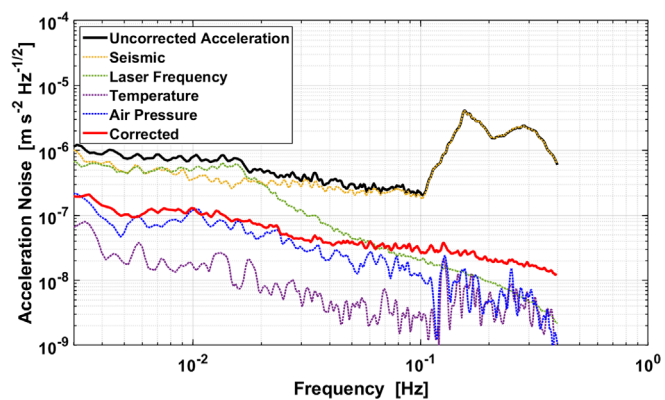
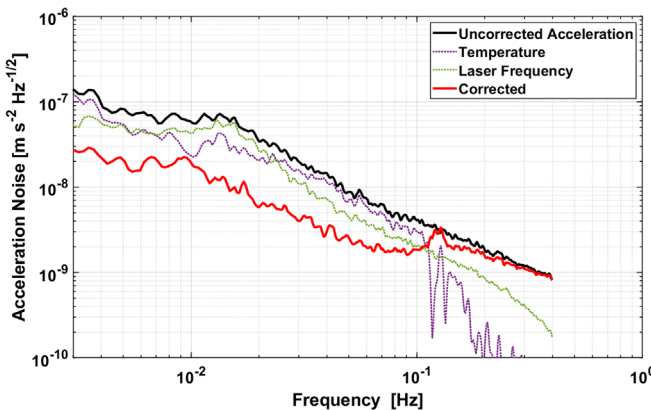


FIG. 5. Acceleration noise budget of a 14-h measurement with our optomechanical accelerometer. Significant noise contributions from ground motion, laser frequency noise, temperature fluctuations, and barometric pressure fluctuations were identified using a combination of linear regression in the time-domain and transfer function estimation in the frequency-domain. Post-correction of these effects lowers the acceleration noise floor to  $10 \text{ nm s}^{-2} \text{ Hz}^{-1/2}$  at 0.4 Hz.



**FIG. 6.** Observed acceleration noise during a 14-h measurement while the test mass was anchored in place. Significant noise contributions from laser frequency noise and temperature fluctuations were identified using a combination of linear regression in the time-domain and transfer function estimation in the frequency-domain. We observe an acceleration noise of  $0.8 \text{ nm s}^{-2} \text{Hz}^{-1/2}$  at 0.4 Hz.

were removed in postcorrection, it is anticipated that the residual noise floor in Fig. 6 is dominated by noise from the free-space quasi-monolithic interferometer and the optical fibers in our setup. These noises are under investigation but could potentially originate from small-vector terms in the fiber optics, which can be mitigated by an active mechanical stabilization of the fibers using a fiber stretcher.<sup>18</sup>

We observe that the free test mass measurement experiences excess noise relative to the anchored measurement. Potentially, this noise is introduced through the post-correction process. As each of our auxiliary sensors have their own respective self-noises, using them to decohere our acceleration measurement inevitably adds those self-noises to our acceleration. This emphasizes that post-correcting data, as we have done in this paper, is not a long-term solution, but an investigation that informs us how to prevent noise from coupling into our measurements in the first place. Temperature and barometric pressure fluctuations can be mitigated by operating in vacuum, while laser frequency noise can be reduced with laser stabilization techniques such as Pound–Drever–Hall locking or phase-offset locking to a stabilized frequency source. This laser frequency noise can also be mitigated by minimizing the distance between the reference and test mass mirrors. Another potential noise source is tilt-to-length coupling in the measurement interferometer arm, which, if significant, could have a larger impact when test mass is moving.

Furthermore, we compare our post-corrected acceleration noise floors to the self-noise of the GS-13 in Fig. 7. We find that in an environment with minimal temperature and pressure fluctuations, such as in vacuum, our optomechanical accelerometer is anticipated to outperform the GS-13 below 1 Hz. As the GS-13 seismometers are the primary instruments for ground motion detection in LIGO gravitational wave detectors, this suggests our optomechanical accelerometer would be an improvement over the sensors currently deployed by LIGO.

In this paper, we present the design of an optomechanical accelerometer composed of a fused silica mechanical resonator whose displacement from equilibrium is measured using a heterodyne laser interferometer. Our optical test mass readout is a custom-made assembly of prisms with a total footprint of  $10 \times 20 \text{ mm}^2$ , which is integrated

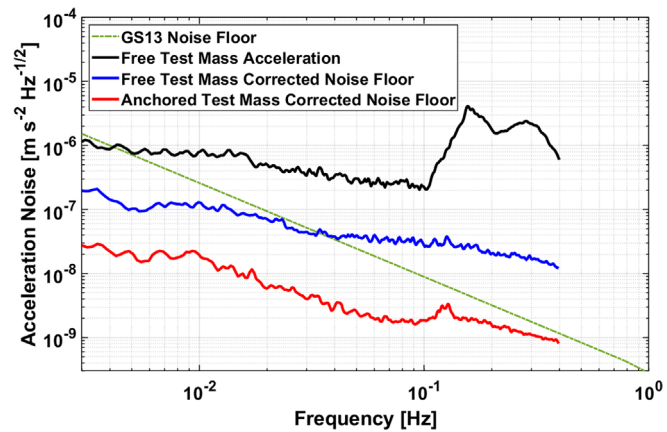


**FIG. 7.** Comparison of our post-corrected acceleration data while the test mass is anchored to calculated thermal acceleration noise floor of our device. Also shown is the self-noise of the GS-13,<sup>17</sup> which is deployed throughout LIGO gravitational wave detectors. We note that our measured acceleration noise floor while the test mass is anchored is better than that of the GS-13 below 1 Hz.

directly onto the fused silica wafer of our resonator. Benchtop measurements taken with this accelerometer demonstrate a noise floor that reaches nano-g  $\text{Hz}^{-1/2}$  sensitivities at 0.4 Hz after correcting for ground motion, air pressure, and temperature effects. When the test mass is anchored in place to prevent ground motion coupling, we demonstrate an acceleration sensitivity of 82 pico-g  $\text{Hz}^{-1/2}$  at 0.4 Hz.

Our optomechanical accelerometer has many advantages over other technologies while maintaining a competitive noise floor. The device presented in this Letter is considerably more compact and lightweight than commercial seismometers, which can weigh more than 10 kg with volumes exceeding 5 l. Consequently, our optomechanical accelerometer is easier to deploy in ground-based and satellite-based applications. Furthermore, commercial seismometers are typically not vacuum compatible, which adds hurdles that must be overcome if they are to be used in certain applications such as ground motion detection in gravitational wave detectors' vacuum chambers. Our accelerometer, on the other hand, is intrinsically vacuum compatible, making it a more practical solution for vacuum applications. For these reasons, we propose the implementation of optomechanical accelerometers for ground motion detection in gravitational wave detectors.

Finally, future generations of gravitational wave detectors including LIGO Voyager<sup>19</sup> and the Einstein Telescope<sup>20</sup> aim to operate at cryogenic temperatures. To this date, however, no acceleration sensing device has been developed that is both cryo-compatible and provides the acceleration sensitivity required for these missions. The work we present in this Letter can be extended to cryogenic applications by a different choice of wafer material. Fused silica is known to lose its low-mechanical loss properties at cryogenic temperatures, which would degrade the performance of a fused silica accelerometer in these conditions.<sup>21</sup> Alternatively, silicon resonators do not suffer from this effect and can retain high  $Q$ -factors in cryogenic applications. Hence, developing an optomechanical accelerometer from silicon based on the same operating principles as the work in this Letter could yield an accelerometer appropriate for use in LIGO Voyager or the Einstein Telescope.

This research was funded by the National Geospatial-Intelligence Agency (NGA) (Grant No. HMA04762010016), National Science Foundation (NSF) (Grant No. PHY-2045579), National Aeronautics and Space Administration (NASA) (Grant Nos. 80NSSC20K1723 and 80NSSC22K0281), and Jet Propulsion Laboratory (JPL) (Contract No.1677619).

## AUTHOR DECLARATIONS

### Conflict of Interest

The authors have no conflicts to disclose.

### Author Contributions

**Adam Hines:** Conceptualization (equal); Data curation (lead); Formal analysis (lead); Investigation (lead); Methodology (equal); Visualization (lead); Writing – original draft (lead). **Andrea Nelson:** Investigation (supporting); Methodology (supporting); Writing – review & editing (supporting). **Yanqi Zhang:** Investigation (supporting). **Guillermo Valdes:** Conceptualization (supporting); Investigation (supporting); Methodology (supporting); Supervision (supporting); Writing – review & editing (equal). **Jose Sanjuan:** Formal analysis (supporting); Methodology (supporting); Supervision (equal); Writing – review & editing (equal). **Felipe Guzman:** Conceptualization (equal); Funding acquisition (lead); Methodology (supporting); Project administration (equal); Resources (equal); Supervision (equal); Writing – review & editing (equal).

## DATA AVAILABILITY

The data that support the findings of this study are available from the corresponding author upon reasonable request.

## REFERENCES

- <sup>1</sup>J. Aasi, B. Abbott, R. Abbott, T. Abbott, M. Abernathy, K. Ackley, C. Adams, T. Adams, P. Addesso, R. Adhikari *et al.*, “Advanced LIGO,” *Classical Quantum Gravity* **32**, 074001 (2015).
- <sup>2</sup>F. A. Acernese, M. Agathos, K. Agatsuma, D. Aisa, N. Allemandou, A. Allocata, J. Amarni, P. Astone, G. Balestri, G. Ballardin *et al.*, “Advanced Virgo: A second-generation interferometric gravitational wave detector,” *Classical Quantum Gravity* **32**, 024001 (2014).
- <sup>3</sup>T. Akutsu, M. Ando, K. Arai *et al.*, “KAGRA: 2.5 generation interferometric gravitational wave detector,” *Nat. Astron.* **3**, 35–40 (2019).
- <sup>4</sup>P. R. Saulson, “Thermal noise in mechanical experiments,” *Phys. Rev. D* **42**, 2437–2445 (1990).
- <sup>5</sup>E. J. Daw, J. A. Giaime, D. Lormand, M. Lubinski, and J. Zweizig, “Long-term study of the seismic environment at LIGO,” *Classical Quantum Gravity* **21**, 2255–2273 (2004).
- <sup>6</sup>D. M. Macleod, S. Fairhurst, B. Hughey, A. P. Lundgren, L. Pekowsky, J. Rollins, and J. R. Smith, “Reducing the effect of seismic noise in LIGO searches by targeted veto generation,” *Classical Quantum Gravity* **29**, 055006 (2012).
- <sup>7</sup>B. P. Abbott, R. Abbott, T. Abbott, M. Abernathy, F. Acernese, K. Ackley, M. Adamo, C. Adams, T. Adams, P. Addesso *et al.*, “Characterization of transient noise in advanced LIGO relevant to gravitational wave signal GW150914,” *Classical Quantum Gravity* **33**, 134001 (2016).
- <sup>8</sup>A. Effler, R. Schofield, V. Frolov, G. González, K. Kawabe, J. Smith, J. Birch, and R. McCarthy, “Environmental influences on the LIGO gravitational wave detectors during the 6th science run,” *Classical Quantum Gravity* **32**, 035017 (2015).
- <sup>9</sup>P. Nguyen, R. Schofield, A. Effler, C. Austin, V. Adya, M. Ball, S. Banagiri, K. Banowetz, C. Billman, C. Blair *et al.*, “Environmental noise in advanced LIGO detectors,” *Classical Quantum Gravity* **38**, 145001 (2021).
- <sup>10</sup>F. Guzmán Cervantes, L. Kumanchik, J. Pratt, and J. M. Taylor, “High sensitivity optomechanical reference accelerometer over 10 kHz,” *Appl. Phys. Lett.* **104**, 221111 (2014).
- <sup>11</sup>A. Hines, L. Richardson, H. Wisniewski, and F. Guzman, “Optomechanical inertial sensors,” *Appl. Opt.* **59**, G167–G174 (2020).
- <sup>12</sup>A. Hines, A. Nelson, Y. Zhang, G. Valdes, J. Sanjuan, J. Stoddart, and F. Guzmán, “Optomechanical accelerometers for geodesy,” *Remote Sens.* **14**, 4389 (2022).
- <sup>13</sup>Y. Zhang and F. Guzman, “Quasi-monolithic heterodyne laser interferometer for inertial sensing,” *Opt. Lett.* **47**, 5120–5123 (2022).
- <sup>14</sup>A. Cumming, A. Heptonstall, R. Kumar, W. Cunningham, C. Torrie, M. Barton, K. Strain, J. Hough, and S. Rowan, “Finite element modelling of the mechanical loss of silica suspension fibres for advanced gravitational wave detectors,” *Classical Quantum Gravity* **26**, 215012 (2009).
- <sup>15</sup>A. Cumming, A. Bell, L. Barsotti, M. Barton, G. Cagnoli, D. Cook, L. Cunningham, M. Evans, G. Hammond, G. Harry *et al.*, “Design and development of the advanced LIGO monolithic fused silica suspension,” *Classical Quantum Gravity* **29**, 035003 (2012).
- <sup>16</sup>K. Numata, S. Otsuka, M. Ando, and K. Tsubono, “Intrinsic losses in various kinds of fused silica,” *Classical Quantum Gravity* **19**, 1697–1702 (2002).
- <sup>17</sup>F. Matichard, B. Lantz, R. Mittleman, K. Mason, J. Kissel, B. Abbott, S. Biscans, J. McIver, R. Abbott, S. Abbott *et al.*, “Seismic isolation of advanced LIGO: Review of strategy, instrumentation and performance,” *Classical Quantum Gravity* **32**, 185003 (2015).
- <sup>18</sup>Y. Zhang, A. S. Hines, G. Valdes, and F. Guzman, “Investigation and mitigation of noise contributions in a compact heterodyne interferometer,” *Sensors* **21**, 5788 (2021).
- <sup>19</sup>R. X. Adhikari, K. Arai, A. Brooks, C. Wipf, O. Aguiar, P. Altin, B. Barr, L. Barsotti, R. Bassiri, A. Bell *et al.*, “A cryogenic silicon interferometer for gravitational-wave detection,” *Classical Quantum Gravity* **37**, 165003 (2020).
- <sup>20</sup>M. Punturo, M. Abernathy, F. Acernese, B. Allen, N. Andersson, K. Arun, F. Barone, B. Barr, M. Barsuglia, M. Beker *et al.*, “The Einstein Telescope: a third-generation gravitational wave observatory,” *Classical Quantum Gravity* **27**, 194002 (2010).
- <sup>21</sup>A. Schroeter, R. Nawrodt, R. Schnabel, S. Reid, I. Martin, S. Rowan, C. Schwarz, T. Koettig, R. Neubert, M. Thürk *et al.*, “On the mechanical quality factors of cryogenic test masses from fused silica and crystalline quartz,” *arXiv:0709.4359* (2007).